A study of asynchronous noise in indoor power line with applications to power line communication

IOP Conf. Series: Journal of Physics: Conf. Series **1330** (2019) 012013 doi:10.1088/1742-6596/1330/1/012013

A study of asynchronous noise in indoor power line with applications to power line communication

R Baishya[1*], B Tiru[1] and U Sarma

[1]Department of Physics, Gauhati University, Guwahati-14, India
[2]Department of Instrumentation and USIC, Gauhati University, Guwahati-14, India

*Email: rubibaishya89@gmail.com

Abstract. Power line channels do not have standard models for noise simulation. As such, study and analysis of different types of noise is imperative to developing channel simulator where communication systems can be tested and optimized for maximum efficiency. This is an indispensable part in developing power line communication systems that uses the available power line as a communication channel. This paper analyzes the asynchronous impulsive noise in indoor power line channels. The experimental setup for noise acquisition is described in detail. It is found that the impulse amplitude and the impulse durations follow the *t-location scale* and the *log-logistic* distribution better than other distribution tested. Such a distribution is easier to handle in terms of random number generation using the inverse cumulative distribution method. This can be used in the random noise simulation of impulsive noise in the generation of overall power line noise for system testing and optimization.

1. Introduction

An important requisite for developing any communication system is the knowledge of the channel noise that governs important communication parameters like the channel capacity and the probability of error or bit error rate [1]. While selecting the digital modulation schemes, the design goals are maximizing the bit rate and resistance to interfering signals and minimizing the symbol error, the transmit power, bandwidth and circuit complexity. This requires an in-depth knowledge of noise before designing the communication system. This requirement cannot be neglected for power line communication (PLC) that uses the available power line (PL) for data communication. The problem with PLC channels is that the PL noise is non-Gaussian and non-white [2] and standard models and techniques cannot be used to represent the noise [2]. As such, an extensive study of the noise is indispensable before using the infrastructure as a communication channel. PL noise is usually categorized into five types [3]: (a) colored background noise (CBGN), (b) narrowband interferences (NBI), (c) periodic impulsive noise that is asynchronous to the mains frequency, (d) periodic impulsive noise that occurs synchronous with the mains frequency and (e) impulsive noise that is non periodic and asynchronous to the ac mains. The noise that is always present in PL having a low power spectral density (PSD) is termed as CBGN and is a summation of noise due to many sources that reach any site due to reflections at the discontinuities present. The NBI are mainly caused by broadcast stations, in medium and short wave broadcast band. The type (c) is mostly caused by switching power supplies. The impulses have a repetition rate between 50 kHz to 200 kHz. The type (d) are mainly caused by switching of rectifier diodes. These impulses have a repetition rate of 50Hz or 100Hz as the mains cycle, of short duration (a few microseconds) and have a PSD which decreases with frequency.

The type (e) is caused by switching transients in the network and has different durations. For efficient communication, it is required that every type is studied and modeled so that the PLC transceivers can be optimized in a simulated channel before using in the field.

This paper focuses on asynchronous impulsive noise found in PL channels. The paper is sectioned as follows. In section 2, a literature review of the modeling techniques of PL noise is presented with the importance of the present work. Section 3 describes the experimental arrangement of noise acquisition and the algorithm used is also described. In Section 4, the acquired impulsive noise is analyzed in detail, mainly the impulse amplitude and the impulse duration. These are suitably fitted by distribution functions. The paper then discusses the results and also presents the probable applications of this and concludes with the main results and future work.

2. Literature review on modeling methods of power line noise

The researcher has introduced many methods to capture the features of PL noise to regenerate when required. The simulation approach for PL noise regeneration can be divided into two domains, namely the frequency domain and time domain approaches [5]. The CBGN regeneration usually depends on the first approach and both the approaches in the analysis of impulsive noise. Some of the methods used in different types of noise are the Middleton's model [6, 7] in case of impulsive noise; concept of noisy load which is affected by the frequency response of the channel [5, 8, 9]; Markov models that correlate the impulsive noise with the time variance with loads ; white noise passage through linear filters with pre-determined constant multipliers [10] and lastly is adding the individual noise types described by the Zimmermann components [11, 12] to develop the overall noise environment. In the Middleton model, the total noise (impulsive and background) is depicted by two parameters; the impulse indexes (A) and the background to impulsive power ratio (Γ)**.** However, this technique was originally developed to model man made interferences, and many researchers are still inconclusive whether the same can be applied to impulsive noise found in PL [7]. The noisy load concept and the Markov model require knowledge of the channel to be known *a-priori* [7-9]. This is however the impossible prerequisite as the PL is loaded with different loads at unpredictable times and shows non deterministic properties. The passage of noise by constant multipliers requires knowledge of large numbers of multipliers. The last technique of adding different types of noises to constitute a realistic noise model is the usual way of developing the noisy PL channel. A block diagram of this technique is shown in figure 1. Here, every component is modelled by empirical formulas and added to give the noise environment. Thus, the power spectral density (PSD) of the CBGN is found to decrease with frequency and usually modelled by a likewise curve [11] and the simulated noise is obtained by passing white noise through this colouring filter. The NBI uses the help of different distribution functions [11] to generate the sinusoids. The synchronous noise uses the cyclo-stationary noise model [13-14] and the impulsive noise by modelling the characteristics of the impulses [11] namely the impulse amplitude, duration/length and the inter arrival time (IAT). Such a pulse which has the required characteristics is then passed through a filter which has a response of the fast Fourier transform (FFT) of the observed impulses. The characteristics of the impulse are usually modelled by suitable distribution fits according to experimental observations and during simulations, random numbers following these distributions are generated so that the simulated pulses have the required characteristics. Table 1 gives some of the characteristics found in papers. As seen from the table, the distributions are not alike in different venues and this necessitates studies in different venues to get an overall picture. For successful simulation of the PL noise, it is a mandate that every component must be modelled carefully to create a realistic channel environment and the success lies in correct depiction of the dependencies of the various components. The impulse amplitude, impulse duration and the IAT also follow complex distributions. Modelling the distribution by complex function makes it difficult to simulate back during the generation process. In this paper, the impulse amplitude and impulse duration has been studied extensively in an indoor PL setting. The parameters are adequately

fitted by suitable distribution that easily enables the same to be regenerated by random number generators. The IAT is left as a future work.

Table 1. Distribution fits of impulse amplitude, duration and IAT

Ref	venue	Distributions		
		t_{amp}	t_d	IAT
14	Indoor	MCA[a]	Random	Markov Chain
14	Indoor	Weibull	Random	Markov Chain
14	Indoor	FSWGP[b]	Random	Markov Chain
15	Industrial/residential	Rayleigh	Random	Not defined
16	Indoor	Exponential	Random	Exponential
17	Indoor	TTG[c], MCA[a]	Random	Exponential
18	Industrial	αStable	ME[d]	Pareto
19	Household	Gaussian	Random	---
19	Household	Weibull	Random	---
19	Household	Log-normal	Random	---
P[e]	Laboratory	*t-location scale*	LL[f]	---

[a] Middleton Class A
[b] Finite sum of weighted Gaussian PDF
[c] Two term Gaussian
[d] Mixed exponential
[e] Present work
[f] *log logistic*

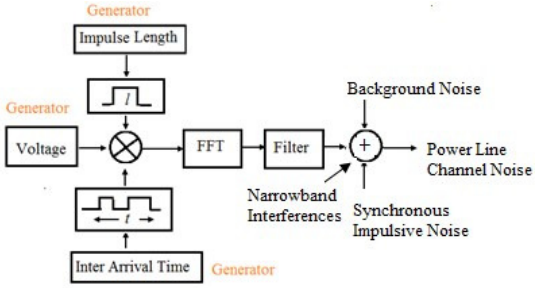

Figure 1. Power line channel noise simulation

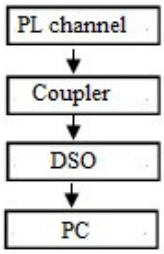

Figure 2. Block diagram of the experimental setup for noise acquisition

3. . Experimental setup for impulse noise acquisition

The block diagram of the impulsive noise acquisition from an indoor PL is shown in Figure 2. It consists of a coupler connected to the phase-neutral line of a PL, a digital storage oscilloscope (DSO) for noise acquisition and a PC for control and perform off line analysis.

3.1. The Coupler

The coupler is a passive high pass filter (HPF) that protects the connected instruments from being harmed by the PL signal. The construction of the coupler is shown in figure 2. It consists of a suitable

1:1 transformer (T) and two capacitors (C1 and C2) so that the frequency response is flat over a broad range of frequencies. The coupler uses differential mode coupling and has galvanic insulation. The latter is caused by inductive coupling of the transformer thereby preventing physical connection to the network. This is safer than capacitive coupling. The high voltage capacitors C1 and C2 are chosen so that the impedance at 50Hz is high. The use of the capacitors in a symmetrical configuration meets the requirement of electromagnetic compatibility (EMC) [20]. The windings of T are bifilar around ferrite cores to enable high frequency noise components to pass un-attenuated. A number of protection measures are used to protect the connected instruments from high voltages like the varistor, FUSE and switching diodes. The latter protects the measuring device from voltage spikes. If there is a voltage spike larger than 2.1V across the output, then diodes D1, D3, D5 will turn on and clip the output voltage. Conversely, if the voltage spike is less than -2.1 V then the diodes D2, D3, D4 will turn on and clip the output voltage. There is also a high watt resistor (PROTECT) that discharges the capacitor and protects users from possible shock. A number of couplers are designed, the specifications of which are given in table 2. The frequency responses of the couplers are shown in figure 3. The cut off frequencies of the couplers range from 25 kHz-150 kHz (Coupler 1, Coupler 2, Coupler 3) with a roll off rate from 30dB/decade- 35dB/decade offering high attenuation to the 50Hz signal. Mostly the 25 kHz coupler was used for impulse noise acquisition.

Table 2. The specifications of the couplers

		Specification and values	
Component	Purpose	Specification	values
FUSE	protection	Glass cartridge	5A, 250V
PROTECT	Protection	Resistor	1MΩ
Varistor	Protection	MOV[a]	385VDC, 7 mm
Diode	Clipping	Switching	IN4148
Coupler-1	HPF	2.38mH[d], 1nF[e]	100kHz[b], 30dB/decade[c]
Coupler-2	HPF	550μH[d], 1nF[e]	150kHz[b], 35dB/decade[c]
Coupler-3	HPF	460μH[d], 100nF[e]	25kHz[b], 35dB/decade[c]

[a] Metal Oxide Semiconductor
[b] Cut off frequency
[c] Roll off rate
[d] Transformer (T)
[e] Capacitor C1 and C2

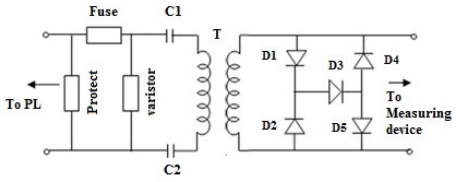

Figure 3. The construction of the coupler

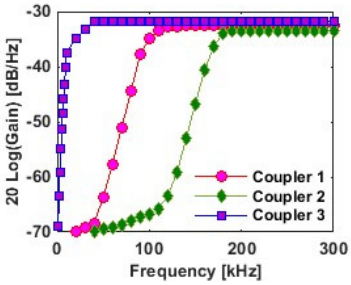

Figure 4. The frequency response of the couplers

3.2. The PC controlled Digital Storage Oscilloscope

The coupler is connected to a DSO (Agilent, 1012A, 2 channel, 100MHz, 2 GS/s) that acquires noise from the phase-neutral pair of an indoor PL in a university building. The loads to the PL were the usual laboratory equipment. The accuracy of the DSO is 8 bits and has a maximum waveform record point of 10^4 points. The DSO is controlled by the Agilent IO library suit software installed in a PC via the MATLAB software. Figure 5 gives the flowchart of the algorithm to acquire noise signal from the PL. At the first stage, a VISA object is created that specifies the vendor, port, buffer size, time out, N etc. of the controlled devices. N is the total number of acquisitions required. Next, commands are given to control the DSO by using the standard command for programmable instruments (SCPI) of the DSO such as the source of the signal to be acquired (channel number), the mode of acquiring, the type and the acquisition mode. The DSO is initially programmed to acquire signal in 'single mode' and the trigger level in the DSO is initially selected as that required. The sampling rate of the DSO is fixed at 50MS/sec. For background noise acquisition, the trigger is selected to be at 80mV as this is the noise floor of the CBGN. For impulsive noise, a trigger value of 110mV is selected. Whenever noise of greater than this trigger level, the trigger status is read and the signal is acquired by the DSO and transferred to the controlling PC. The data file consists of a time stamp, a data stamp and also the actual data. After acquisition ends, the DSO is again set for 'single acquisition' mode. This loop continues till the required number of impulses N is obtained. As there is a delay for the overall operation to be completed in a single impulse, the IAT cannot be found out using the time stamp as

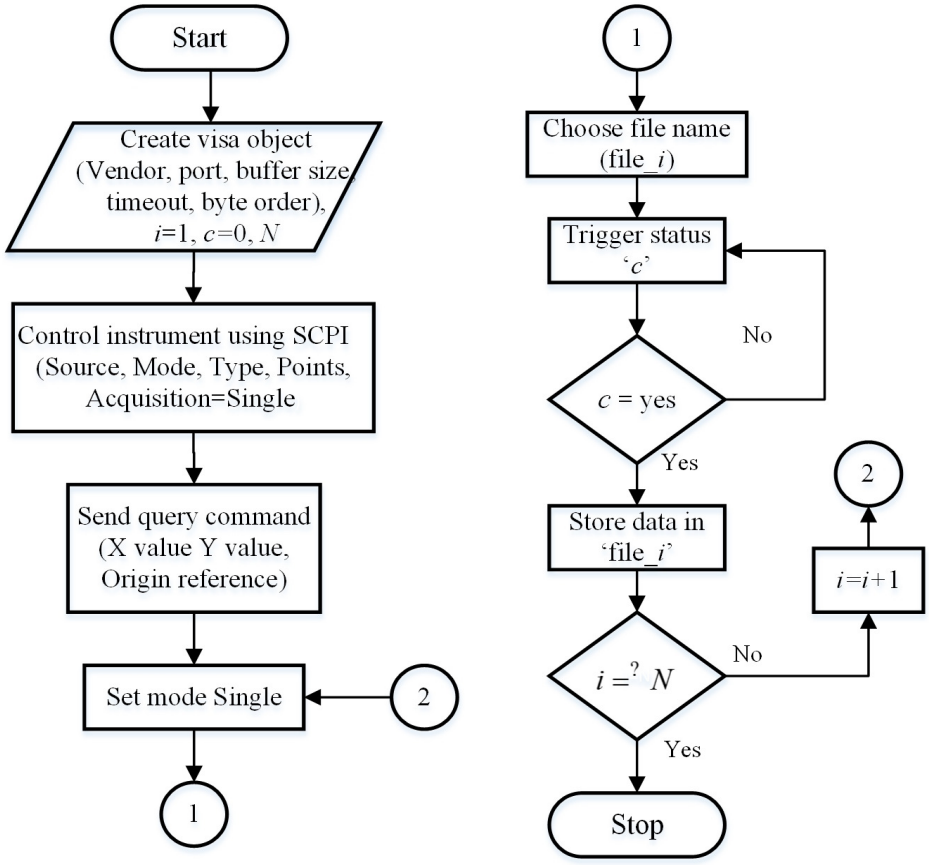

Figure 5. The flowchart for programming the DSO for impulsive noise

the same can be of microsecond level. This signal is then analysed offline. The system is allowed to operate for one week duration and the total number of impulses recorded was nearly 1000Synchronous noise and NBIs was absent in the site. The acquired impulses are analysed offline.

4. Analysis of asynchronous impulsive noise in indoor power line channels

In this section, an analysis of the acquired asynchronous impulsive noise is done.

4.1. The impulsive noise characteristics

A typical impulsive noise is shown in figure 6. The impulse is designated by its impulse length or impulse duration (t_d), the impulse amplitude and the IAT or t_{arr}. The impulse length is the duration for which the impulse remains. The IAT is the time between two impulses. Here, an analysis of amplitude and length is done.

4.2. The power spectral density of the impulses

The PSD of the asynchronous impulsive noise is shown in figure 7. As seen from the figure, the noise is non white and increases the noise floor to as much as 20dB. The PSD of the impulsive noise usually effects the low frequency range <1MHz. The figure also shows the plot of the PSD of the CBGN.

4.3. The statistics of the impulse amplitude and length

The distribution of the parameters of the impulse characteristics, necessarily the impulse amplitude and duration/length are found out. For this, different types of distribution, like *t-location scale*, *log-logistic*, *log-normal* etc. are considered. The maximum *log likelihood* method is used to test the best fit of the distributions. Table 3 and table 4 gives the likelihood parameters (*NlogN*) for the distributions tested. Figure 8 and 9 give the distribution for the different parameters.

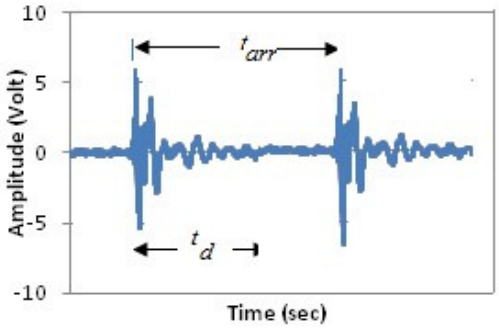

Figure 6. The characteristics of impulsive noise

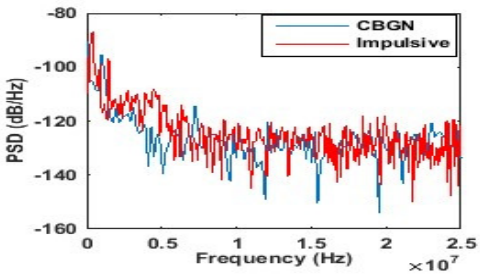

Figure 7. The FFT of impulsive noise compared against the background noise

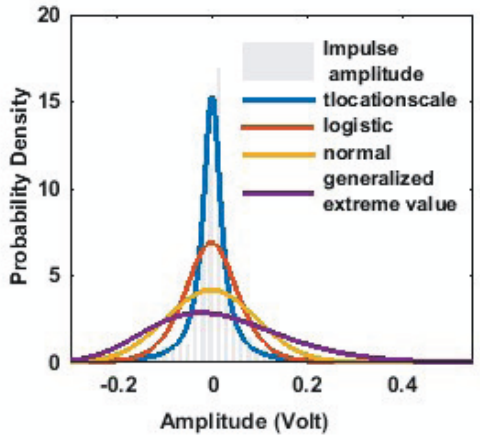

Figure 8. The probability distribution of impulse amplitude for different fits

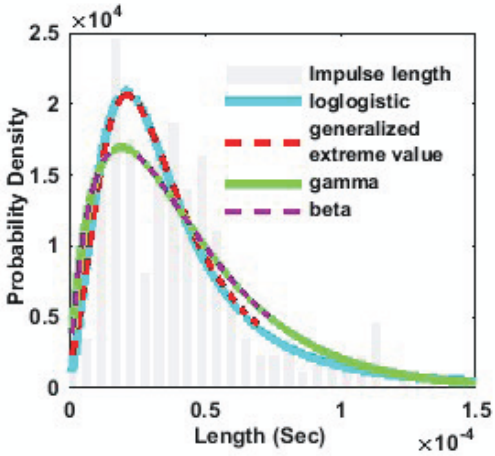

Figure 9. The probability distribution of impulse length for different fits

5. Results and Discussion

In this work, the best fit distribution of the impulse amplitude is found to be *t-location scale* (table 2). The *t-location scale* distribution function has heavier tails than the Gaussian distribution and the probability density function (PDF) is given by equation (1)[21].

$$f(x) = \frac{\Gamma\left(\frac{\nu+1}{2}\right)}{\sigma\sqrt{\nu\pi}\,\Gamma\left(\frac{\nu}{2}\right)}\left[\nu + \frac{x-\mu}{\sigma}\right]^{-\left(\frac{\nu+1}{2}\right)} \qquad (1)$$

In equation (1), Γ is the Gamma Function, σ is known as the scale parameter, ν is the space parameter and μ is the location parameter. σ gives a measurement of the statistical dispersion of the probability distribution. Table 3 shows that the *generalized extreme values (GEV)* is the best fit for the impulse duration. However, in the simulation, the *log logistic* can be more convenient in regard to the Zimmermann technique of noise simulation. The *log-logistic* distribution is a two parameter distribution specified by the scale parameter (μ) and shape parameter (σ) as given by

$$f(t) = \frac{e^{z}}{\sigma t\left(1+e^{z}\right)^{2}}, \qquad (2)$$

where

$$z = \frac{t'-\mu}{\sigma} \qquad (3)$$

$$t' = \ln(t) \qquad (4)$$

where $0 < t < \infty,\ -\infty < \mu < \infty$ *and* $0 < \sigma < \infty$

Modelling the impulse amplitude and the impulse duration by these two distributions can easily enable the random number generation by the inverse cumulative distribution function (ICDF) also termed as

inverse transform sampling. In this method, if U is a random number that is uniform and, in the range (0, 1), then the ICDF of the desired distribution applied to U will generate a set of the random numbers V. These new set of random numbers will have the desired distribution. Thus, if F is the cumulative distribution function (CDF) of the desired distribution, then using the non-linear transformation $V= F^{-1}(U)$ generates the necessary samples satisfying the required distribution. Figure 10 and figure 11 give the distribution of the generated data using this method. The (μ, σ, ν) of the simulated data for impulse amplitude having *t-location scale* distribution is given by (-0.0034, 0.0210, 1.2573) and the (μ, σ) for *log-logistic* distribution for impulse duration is given by (-10.516, 0.4476). It is seen that the generated data has nearly the same distribution to the experimentally observed. Generation of the impulse amplitude and impulse duration having the required distribution will enable simulation of impulses with the observed distribution in the regeneration of the noise components of Zimmermann model.

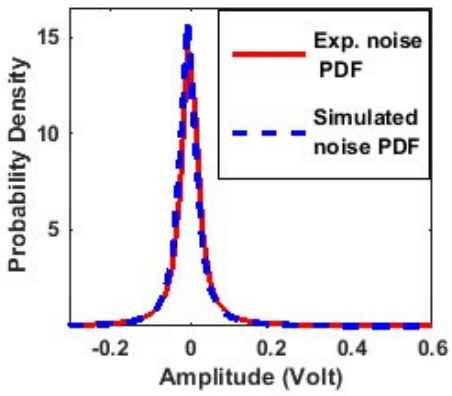

Figure 10. Comparison of the *t-location scale* distribution of the impulse amplitude obtained using the experimental and simulated data.

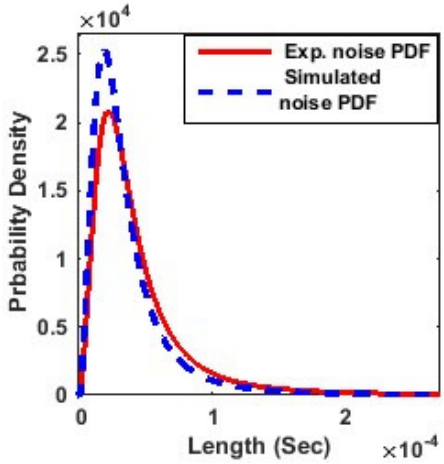

Figure 11. Comparison of the *log-logistic* distribution of the impulse duration obtained using the experimental and simulated data.

Table 3. Distribution fits of impulse amplitude

		Parameters name and values	
Distribution	*NlogN*	name	values
t-location scale	$3.4\text{x}10^5$	location (μ)	-0.0010
		scale (σ)	0.0214
		DOF[a] (ν)	1.1868
logistics	$2.828\text{x}10^5$	location (μ)	-0.0025
		scale (σ)	0.0361
Normal	$2.158\text{x}10^5$	location (μ)	-0.0029
		scale (σ)	0.0955
GEV[b]	$1.662\text{x}10^5$	shape (k)	-0.1397
		location (μ)	0.1296
		scale (σ)	0.0430

[a] Degrees of freedom
[b] Generalized extreme values

Table 4. Distribution fits of impulse length

		Parameters name and values	
Distribution	*NlogN*	name	values
Log-logistic	1.4741×10^3	location (μ)	-10.3272
		scale (σ)	0.4519
GEV[a]	1.4751×10^3	Shape (k)	0.2782
		location (μ)	2.5750×10^5
		scale (σ)	1.8476×10^5
Gamma	1.4724×10^3	Shape (k)	1.8070
		scale (σ)	2.3717×10^5
Beta	1.4724×10^3	shape (k)	1.8069
		scale (σ)	4.216×10^4

[a] Generalized extreme value

6. Conclusion

In this paper, an analysis of the characteristics of asynchronous impulsive noise in indoor PL channels is done. An experimental arrangement is described elaborately that enables the impulses to be captured. The analysis shows that the characteristics can be fitted with suitable models, the ICDF of which can easily help regenerate the noise. The arrangement, however does not allow the IAT to be captured due to the time delay in a single acquisition process of the DSO. Suitable arrangements are required for removing this shortcoming. Such noise generation will improve the replication of the PL channel in software that will enable optimization of PLC devices before implementing in hardware and testing in field. In the future, the impulse characteristics including the IAT will be studied in a number of sites and a more in-depth analysis will be made using the experimental arrangement.

References

[1] Galli S, Scaglione A and Wang Z 2011 *Proc. IEEE* **99(6)** 998
[2] Zimmermann M and Dostert K 2002 *IEEE Trans. Electromagn. Compat.* **44 (1)** 249
[3] Zimmermann M and Dostert K 2000 *Proc. Int. Symp. on Power Line Communication and its Applications* p131
[4] Meng H, Guan Y L and Chen S 2005 *IEEE Trans. Power Del.* **20 (2)** 630
[5] Andreadou N and Pavlidou F N 2010 *IEEE Trans. Power Del.* **25(1)** 150
[6] Najarkolaei A H, Hosny W, Lota J 2015 *Proc. 17th UKSim-AMSS Int. Conf. on Modelling and Simulation (UKSim) (Cambridge, UK)* p248
[7] Sancha S, Cantete F J and Entrambasaguas J. T 2007 *Proc. IEEE Int. Symp. on Power Line Communications and Its Applications* (Pisa, Italy) p 104
[8] Canete Corripio F J, Diez del Rio L, Entrarnbasaguas and Munoz J. T 2001 *Proc. Int. Symp. on Power Line Communications (ISPLC'01)* (Malmo, Sweden) p 85
[9] Phillips H 1999 *Proc. 3rd Int. Symp. Powerline Communications and its Applications* (Lancaster, UK) p 14
[10] Bert L D, Caldera P, Schwingshack D and Tonello A M 2011 *Proc. IEEE Int. Symp. Powerline Communications and its Applications* (Udine, Italy) p 283
[11] Benyoucef D 2003 *Proc.7th Int. Symp. Powerline Communications and its Applications* (Kyoto, Japan) p 136
[12] Nassar M, Dabak A., Kim I, T. Pande and Evans B 2012 *Proc. IEEE Int. Conf. on Acoustics, speech and signal processing, ICASSP* (Kyoto, Japan) p 3089

[13] Xiao Y, Zhang J, Pan F and Shen Y 2016 *J. Circuits Syst.Com.* **25(9)** 1650105
[14] Umehara D, Shinji H, Denno S and Yoshiteru M 2006 *Proc. Int. Symp. on Information Theory and its Applications, ISITA* (Seoul, Korea) p 195
[15] Chan Morgan H L, and Robert W. Donaldson 1989 *IEEE Trans. Electromagn. Compat.* **31(3)** 320
[16] Andreadou N, and Pavlidou F N 2009 *IEEE Trans. Power Del.* **25 (1)** 150
[17] Bert D, Caldera L P, Schwingshackl D and Tonello A M 2011 On noise modeling for power line communications, *Proc. 2011 IEEE Int. Symp. on Power Line Communications and its Applications* p 283
[18] Tran Trung H., Dung D. Do, and Huynh T H 2013 *Int. J. Comp. Elec. Eng.***5 (1)** 48
[19] Jaroslav K and Zeman T 2014 *Adv. in Elec. and Elect. Eng.* **12 (1)** 20
[20] Downey WJ, Sutterlin P Power line communication tutorial -challenges and technologies. https://www.coursehero.com/le/16006749/PLApps- Studywos
[21] Matsumoto EY and Del-Moral-Hernandez E 2013 *Proc. Int. Joint Conf. on Neural Networks,* ICJNN (Dallas, USA) p 1